

## ***CDC42BPA::BRAF* represents a novel fusion in desmoplastic infantile ganglioglioma/desmoplastic infantile astrocytoma**

**Maria Isabel Barros Guinle, Jeffrey J. Nirschl, Yao Lulu Xing, Ella A. Nettnin, Sophia Arana, Zhi-Ping Feng, Emon Nasajpour, Anna Pronina, Cesar A. Garcia, Gerald A. Grant, Hannes Vogel, Kristen W. Yeom<sup>‡</sup>, Laura M. Prolo<sup>†</sup>, and Claudia K. Petritsch<sup>†,•</sup>**

All author affiliations are listed at the end of the article

**Corresponding Author:** Claudia K. Petritsch, PhD, Department of Neurosurgery, Lorry I. Lokey Stem Cell Research Building, G1169, 265 Campus Drive, Stanford, CA 94305, USA ([cpetri@stanford.edu](mailto:cpetri@stanford.edu)).

<sup>†</sup>Equal contribution.

<sup>‡</sup>Present Address: Department of Radiology, Phoenix Children's Hospital Thomas Campus, Phoenix, USA.

**Desmoplastic infantile ganglioglioma/desmoplastic infantile astrocytoma (DIG/DIA) are low-grade glial/glioneuronal tumors occurring predominantly in the cerebral hemispheres of infants. DIG/DIA exhibit *BRAF* or *RAF1* alterations leading to oncogenic mitogen-activated protein kinase (MAPK) pathway activation. Here, we report the discovery of the novel *CDC42BPA::BRAF* fusion in a 3-month-old patient with left frontotemporal DIA using DNA sequencing. Independent validation was performed through RNA sequencing. This fusion joins the kinase domains of *BRAF* and *CDC42BPA*, potentially constitutively activating both. It marks the first report of a fusion involving the actomyosin regulatory kinase *CDC42BPA/MRCKα* in brain tumors, suggesting the potential involvement of actin remodeling defects in DIG/DIA. Surgical excision is curative for DIG/DIA, but incomplete resection, recurrence, malignant transformation, or metastases may necessitate adjuvant chemotherapy, posing risks. Identifying and excluding molecular alterations is crucial for selecting targeted therapies, such as *BRAF* and *MEK* inhibitors. These options present potential treatments with lower toxicity compared to conventional chemotherapy.**

Desmoplastic infantile ganglioglioma (DIG) and desmoplastic infantile astrocytoma (DIA) are benign tumors composed of a mixed astrocytic and neuronal component (DIG) or an astrocytic component (DIA).<sup>1</sup> DIG/DIA are typically cured with surgical excision, with no further treatment needed.<sup>1</sup> However, in cases of subtotal resection, recurrence, malignant transformation, or metastases, adjuvant treatment typically consisting of chemotherapy is used, which can contribute to morbidity and mortality.<sup>2</sup> DIG/DIA exhibit oncogenic activation of the mitogen-activated protein kinase (MAPK) pathway particularly due to mutations in *BRAF* and *RAF1*, 2 genes encoding central pathway kinases. Receptor tyrosine kinase fusions common in infant-type hemispheric glioma and consistent recurrent

chromosomal alterations are not found in DIG/DIA.<sup>3-7</sup> Therapy targeting the MAPK pathway include inhibitors of p.V600E *BRAF*, p.V600E wild-type *BRAF*, and *MAPK*. These inhibitors are already in clinical use or actively in clinical development against gliomas ([Supplementary Table S1](#)). Thus, it is critical to identify specific molecular alterations within the MAPK pathway, as it may enable the use and inform the choice of such targeted therapies for treatment of clinically challenging DIG/DIA.

Here, we utilized DNA sequencing to discover and RNA sequencing to validate a novel *CDC42BPA::BRAF* fusion in a 3-month-old patient diagnosed with DIA. This fusion highlights a previously unreported alteration in which 2 kinase-encoding genes *BRAF* and *CDC42BPA*, are predicted to be fused. The fusion event joins the kinase domains and releases the auto-inhibitory domains of *BRAF* and *CDC42BPA*, raising the possibility that both kinases and their respective downstream pathways are activated by the fusion event. This discovery also marks the first report of a fusion event involving *CDC42BPA*, the gene encoding the serine/threonine kinase *CDC42BPA* also known as myotonic dystrophy kinase-related *CDC42*-binding kinase isoform alpha (*MRCKα*) in brain tumors. This finding is important because *CDC42BPA* is not included in routine gene panels used to analyze cancer genomes. Besides the upregulation of the MAPK pathway, our findings suggest a potential involvement of *CDC42BPA/MRCKα* activity-driven cell motility in DIG/DIA.<sup>8</sup>

### **Case Presentation and Clinical Course**

A 3-month-old, male patient presented to the emergency department with a new onset of generalized tonic-clonic seizures. A computed tomography scan of the head revealed

a left frontal mass with 11 mm midline shift and surrounding vasogenic edema. Further evaluation with magnetic resonance imaging (MRI) showed a solid and cystic left frontotemporal mass concerning for DIG/DIA, glioma, ependymoma, or embryonal tumor (Figure 1A–C). The patient underwent surgical resection, and a postoperative MRI revealed gross total resection (Figure 1D–F). Follow-up brain MRI at 1 year showed resolution of midline shift and no evidence of recurrence (Figure 1G–I).

## Standard and Molecular Diagnostic Testing

### Targeted Illumina Shotgun Sequencing With the Stanford Solid Tumor Actionable Mutation Panel (STAMPseq)

The patient's family consented to tumor specimen donation under Stanford Institutional Review Board approval. Targeted Illumina shotgun sequencing was performed on paraffin-embedded tissue using the Stanford Solid Tumor Actionable Mutation Panel (STAMP). STAMP sequencing (STAMPseq) provides full exonic coverage for 197 genes to detect single nucleotide variants, short insertions and deletions, and selected gene fusions. Genomic positions are given in reference to the GRCh37 (hg19) assembly of the human genome (Supplementary Table S2). STAMPseq identified a novel *CDC42BPA::BRAF* fusion with breakpoints in intron 14 of *CDC42BPA* and in intron 10 of *BRAF* (Figure 2A; Supplementary Table S3). The resulting fusion is predicted to yield an in-frame fusion of *BRAF* at exon 11 and *CDC42BPA* at exon 14. The fusion includes the entire *BRAF* kinase domain and results in the loss of the N-terminal auto-inhibitory domain, which is predicted to activate *BRAF* and downstream MAPK signaling.<sup>9</sup> The fusion includes exon 1–14 of the *CDC42BPA/MRCKα* gene, whereby exon 1 encodes the ATG initiation codon and a conserved domain important for kinase domain dimerization and kinase activation. Exons 2–9 encode the entire kinase domain of *CDC42BPA/MRCKα* and exons 10–14 encode the first 5 exons of the extended coiled-coil domain (Figure 2A). The truncated protein lacks the auto-inhibitory distal coiled-coil domains and binding domains for *CDC42-GTP*.<sup>10</sup> No other pathogenic or likely pathogenic alterations were identified by STAMPseq. The estimated tumor mutation burden was 1.1 Mutations/Mb.

We subsequently verified these findings through a re-analysis of the STAMPseq data by extracting the paired-end reads and aligning them to a different human reference genome (GRCh38/hg38) than the one utilized in the initial analysis, using the raw STAMPseq data and the *bwa-mem2* aligner. The read depths from STAMPseq were determined at approximately 20 million paired-end reads, each 150 base-pair (bp) in length. The *CDC42BPA::BRAF* fusion was validated and visually confirmed using the Integrated Genome Viewer. The reads mapped in intron 14 of the *CDC42BPA* gene paired with those mapped in intron 10 of the *BRAF* gene (Figure 2B; Supplementary Table S3) with breakpoints at Chr1: 227 110 644 and Chr7: 140 782 790, respectively. The difference in the loci between the 2 STAMPseq analyses is due to the alignment

against different reference genomes (Supplementary Material; Figure 2B; Supplementary Tables S2, S3).

This result successfully replicated the identification of the novel *CDC42BPA::BRAF* fusion and the predicted linking of the kinase domains of *BRAF* and *CDC42BPA/MRCKα*.

### RNA Sequencing, STAR-Fusion, and FusionInspector

We performed whole-transcriptome RNA sequencing (RNAseq) to independently verify the presence of the *CDC42BPA::BRAF* fusion. Paired-end sequences were aligned using the *hisat2* and *STAR* software, demonstrating unique and concordant mapping to the reference genomes GRCh38/hg38 (Supplementary Table S2). Leveraging *STAR-Fusion*, we effectively confirmed that the fusion is present within the tumor sample. We employed *FusionInspector* for *in silico* evaluation of the predicted fusion transcript, and used *Integrated Genome Viewer* for visualization, collectively providing independent validation for the novel *CDC42BPA::BRAF* fusion.<sup>11</sup> Notably, the results confirm the fusion occurs between the last base of exon 14 of *CDC42BPA* and the first base of exon 11 of *BRAF* (Supplementary Material; Figure 2C; Supplementary Tables S2, S3).

In contrast to STAMPseq, RNAseq technology captures sequences of transcribed RNA molecules in cells, meaning the reads from mature mRNA transcripts exclude introns. Consequently, the breakpoints highlighted in Figure 2C correspond to transcribed regions of the *CDC42BPA::BRAF* fusion.

Taken together, the predicted fusion protein links the kinase domains of *BRAF* and *CDC42BPA/MRCKα*, consistent among RNA and STAMP sequencing data.

### Methylation Profiling

To classify the tumor independently, we performed DNA methylation profiling of the patient tumor at the National Cancer Institute.<sup>12</sup> The DNA methylation analysis indicated a match to the "DIG/DIA" class using the NCI-EPIC brain classifier with a high confidence score of 1 (out of 1; with a high confidence score  $\geq 0.85$ ), and the German Cancer Research Center (DKFZ) Heidelberg Brain Classifier (v12.5, MolecularNeuroPathology.org). Additionally, UMAP dimensionality reduction analysis clustered the sample within the "DIG/DIA" type. The inferred copy number analyses from DNA methylation profiling show a flat copy number variation profile and found no indications of substantial large chromosomal alterations, amplifications, or deletions in the analyzed data, consistent with earlier molecular evaluations (Supplementary Figure S1).<sup>4,5,7</sup> Additionally, there were no significant genomic losses observed in specific chromosome regions, and no gain of genomic material corresponding to *MET*, *PDGFR*, and *MDM2* genes, as previously reported in other DIG/DIA cases (Supplementary Figure S1).<sup>4</sup>

### Histopathologic Findings Compatible With DIA

Histological sections showed a proliferation of spindled glial cells within a desmoplastic, collagenous stroma

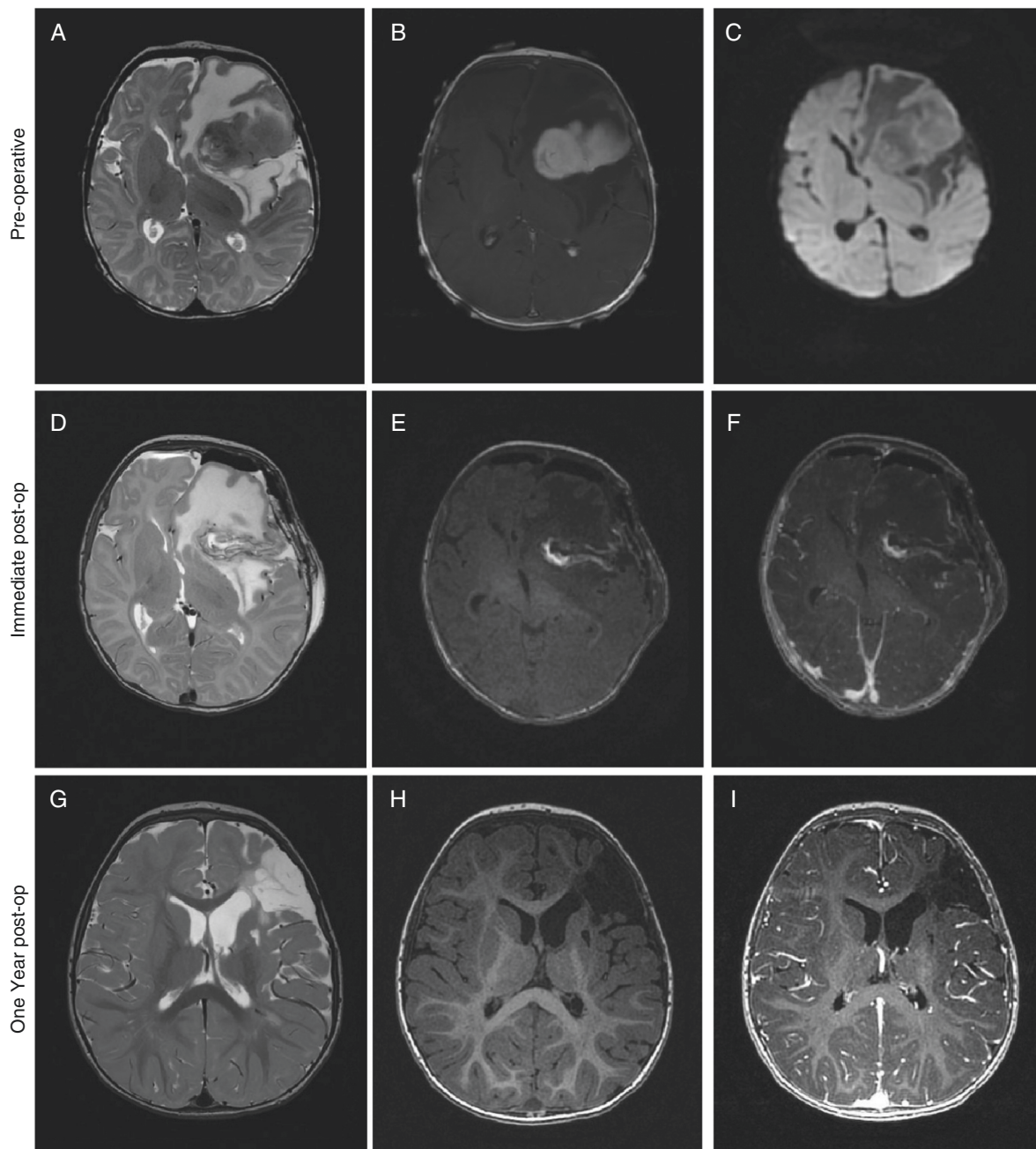


**Figure 1.** Radiologic features indicative of desmoplastic infantile ganglioglioma (DIG)/desmoplastic infantile astrocytoma (DIA). Preoperative axial T2 weighed magnetic resonance imaging demonstrates a  $3.9 \times 4.8 \times 5$  cm solid and cystic left frontotemporal mass with extensive surrounding vasogenic edema and 11 mm of midline shift (A). Axial T1 with contrast shows the lesion contrast enhances (B) and diffusion-weighted sequences show the lesion does not diffusion restrict (C). Imaging characteristics and age of patient favor DIG/DIA (DIG/DIA), less likely glioma, ependymoma, or embryonal tumor. Immediate postoperative (post-op) axial T2 (D), T1 without contrast (E), and T1 with contrast (F) show gross total resection of the lesion. One-year post-operative (post-op) axial T2 (G), T1 without contrast (H), and T1 with contrast (I) show no evidence of tumor recurrence.

arranged in a fascicular to storiform pattern (Figure 3A, B). Occasional gemistocytes were seen but no small cell or immature components, mitotic activity, or necrosis (Figure 3A, B, and H). A trichrome stain highlighted the collagen-rich matrix, while reticulin staining displayed dense pericellular basal lamina deposition (Figure 3C, D).

The predominance of astrocytic differentiation as demonstrated by staining for glial fibrillary acid protein without significant ganglion cells by morphology (Figure 3H) or immunohistochemistry for Synaptophysin (Figure 3F, G) and NeuN (data not shown) was most compatible with DIA.<sup>1</sup>

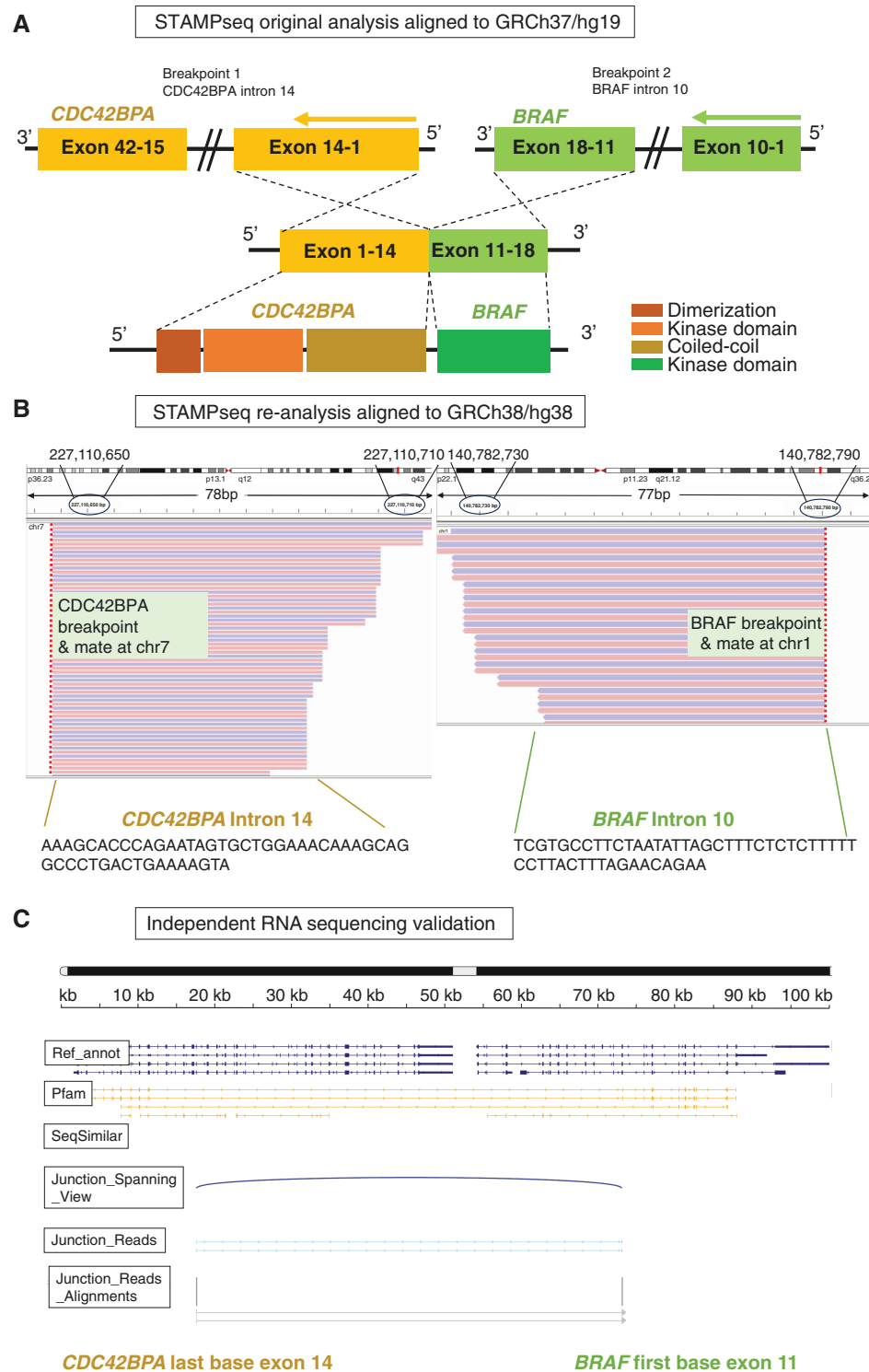


**Figure 2.** Identification and validation of the novel *CDC42BPA::BRAF* fusion. Original analyses of targeted exome sequencing (STAMPseq) of the patient tumor tissue aligned to reference genome GRCh37/hg19 revealed a *CDC42BPA::BRAF* fusion. The predicted numbers correspond to exons (A). STAMPseq re-analysis and alignment to reference genome GRCh38/hg38 confirmed the presence of the *CDC42BPA::BRAF* fusion gene. Data were visualized in the Integrated Genome Viewer after read alignment to the human reference genome GRCh38/hg38 using bwa-mem2. The reads mapped in Chr1: 227 110 626—227 110 735 intron 14 of *CDC42BPA* gene paired with those mapped in Chr7: 140 782 695—140 782 803 intron 10 of *BRAF* gene, with breakpoints at Chr1: 227 110 644 and Chr7: 140 782 790, respectively. The read coverage is 30 for *BRAF* and 74 for *CDC42BPA* of the *CDC42BPA::BRAF* fusion. Pink lines indicate reads mappable in forward direction in 5'-end (R1). Purple lines indicate reads mappable in reverse direction (R2; B). Independent RNA sequencing validation of the fusion. Screenshot of FusionInspector from RNAseq data referenced with the human reference genome GRCh38/hg38. The fusion occurs between the last base of exon 14 of *CDC42BPA* (NM\_001366011.1, chr1:227 112 312) and the first base of exon 11 of *BRAF* (NM\_00137874.1, chr7:140 781 693). As the reads from RNAseq are from mature mRNA transcripts, the breakpoints indicated were corresponding transcribed regions of the *CDC42BPA::BRAF* fusion (C).

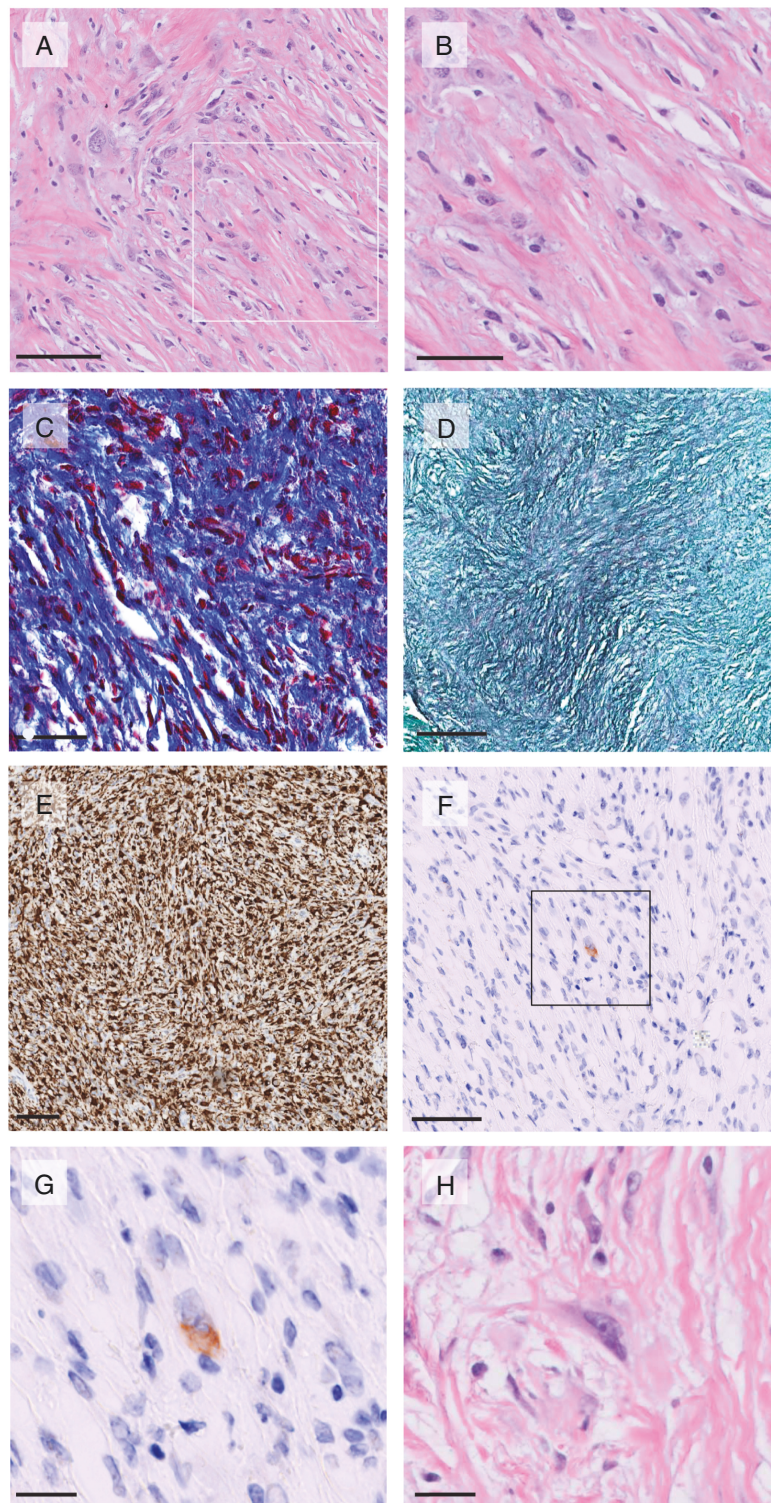


**Figure 3.** Histopathologic features indicative of desmoplastic infantile astrocytoma. Neoplastic astrocytic tumor stained with hematoxylin & eosin (H&E) shows spindle cells and glial cells arranged in a storiform pattern and embedded in a collagen-rich desmoplastic stroma (A), and a higher magnification of the area outlined with a square in (A) showing the absence of mitotic cells (B). Masson's trichrome demonstrates the collagenous stroma in blue (C). Reticulin fibers (black) indicate the basal lamina surrounding tumor cells (D). Glial fibrillary acidic protein highlighting the astrocytic tumor component (E). Synaptophysin labels rare, isolated cells at lower (F), and higher magnification of the area outlined with a square (G). H&E staining confirmed that focally, there were rare ganglion-like cells, but the vast majority of tumor was astrocytic with no ganglion cells by morphology (H). Scale bars = 100  $\mu$ m in (C, D, and E); Scale bars = 50  $\mu$ m in (A and F); Scale bar = 20  $\mu$ m in (B, G, and H).

## Discussion

DIG/DIA are rare, low-grade glial/glioneuronal tumors of infancy-early childhood. The most common oncogenic event in DIG/DIA is MAPK pathway activation caused by mutation or fusion involving *BRAF* or *RAF1*.<sup>3</sup> Somatic mutations in *BRAF* and *RAF1* include the common *BRAF V600E* and the extremely rare *BRAF V600D*, in addition to a *BRAF* indel mutation involving codons 600–604.<sup>3,5</sup> Whereas fusions such as *FXR1::BRAF* and *PRKAR2A::RAF1* are reported in DIG/DIA, the *KIAA1549::BRAF* fusion of pilocytic astrocytoma is not.<sup>5,7</sup> Oncogenic *BRAF* fusions are created by genomic rearrangements leading to the replacement of the auto-inhibitory domain of *BRAF* and placing the 3' portion of the *BRAF* gene encoding the kinase domain behind portions of another gene at the 5' position. Expression of *BRAF* fusion oncoprotein is controlled by the promoter of the 5' fusion partner and leads to constitutive activation of the *BRAF* kinase and downstream MAPK pathway.<sup>9</sup>

In this report, we introduce a novel *CDC42BPA::BRAF* fusion not yet documented in the Fusion Gene Annotation Database (FusionGDB)<sup>13</sup> or the TCGA Fusion Gene Database.<sup>14</sup> This fusion contains kinase domains of *BRAF* and *CDC42BPA/MRCKα* and lacks the respective auto-inhibitory domains, which raises the possibility that both kinases are active and contribute to tumorigenesis. Kinase assays aimed at assessing the activity of the fusion protein will ascertain whether the truncated and fused kinase domains exhibit higher activity levels compared to their respective full-length kinases. *CDC42BPA/MRCKα* has been implicated in several cancer types, including glioblastoma as a crucial regulator of cell proliferation, migration, and invasion, and small molecule inhibitors have been developed, highlighting the emerging potential of these kinases as anticancer targets.<sup>8</sup> As the first report of a fusion between *CDC42BPA* and another gene in brain tumors it suggests a potential role of *CDC42BPA/MRCKα* in DIA.

Although our case shows DIA histology, the histological distinction between DIA/DIG may be less relevant, as studies have reported that DIA and DIG share similar genetic alterations and epigenetic profiles, in addition to common clinical features such as onset at a median age of 1 year, as well as similarities in radiological, and histological aspects, suggesting they may represent a spectrum of morphologic variation of a single molecular tumor type.<sup>15</sup>

A 'wait and watch' approach is typically recommended with complete surgical resection, for patients with DIG/DIA. Our patient's tumor showed no alterations in *TP53*, *ATRX*, or *BCORL1*, which have been seen in cases of recurrence or malignant transformation.<sup>1,7</sup> We have a patient follow-up for over 1 year without radiologic signs of residual tumor or recurrence, but the molecular information provided by 2 independent methods (next-generation DNA sequencing and RNA sequencing) will be relevant for future therapy planning, if needed. In cases of residual tumors or recurrences, identifying molecular targets involved in the MAPK pathway activation can offer opportunities for rapid translation since several *BRAF* and *MEK* inhibitors are

available for clinical use, generally well-tolerated and effective in children. Dabrafenib and trametinib, a combination of *BRAF* and *MEK* inhibitors, have recently received FDA approval for the treatment of low-grade gliomas with *BRAF V600E* in patients aged 1 year and older who require systemic treatment. Encouraging tumor responses have been reported with the *BRAF* inhibitor vemurafenib in patients with *BRAF V600E*-altered DIG/DIA.<sup>3,6</sup> The molecular results for the presented case rule out targeted therapy with *BRAF V600E* inhibitors, and raise consideration for p.V600E wild-type *BRAF* kinase inhibitors and *MAPK* inhibitors, such as trametinib, cobimetinib, and binimetinib. Numerous clinical trials are either ongoing or planned for pediatric low-grade glioma, including DIG/DIA, with many evaluating drugs targeting the *MAPK* signaling pathway (Supplementary Table S1).

Collectively, the data emphasize the importance of identifying and classifying molecular alterations in the *MAPK* pathway in DIG/DIA, as they may enable the use of specific *BRAF* and *MEK* inhibitors in patients that require adjuvant treatment. As molecular diagnostics become more widely used, we can anticipate an increase in discovery of alterations in *CDC42BPA/MRCKα*. With continued advancement in *CDC42BPA/MRCKα* inhibitors,<sup>8</sup> we anticipate substantial and targeted improvements in outcomes for DIG/DIA patients requiring adjuvant treatment.

## Supplementary material

Supplementary material is available online at *Neuro-Oncology* (<https://academic.oup.com/neuro-oncology>).

## Keywords

*CDC42BPA* (*MRCK*) gene alteration | desmoplastic infantile astrocytoma | *MAPK* pathway activation and inhibition | novel *CDC42BPA::BRAF* fusion

## Funding

Botha Family *BRAF* Low-Grade Glioma Consortium and Human Cancer Model Initiative by the National Cancer Institute (C.K.P). Shurl and Kay Curci Foundation, Stanford Maternal & Child Health Research Institute, and Chambers-Okamura Faculty Scholar in Pediatric Neurosurgery (L.M.P.). JJN received support from the National Institutes of Health (NIH) grant P30AG066515.

## Conflict of interest statement

The Authors declare no conflicts of interest in relation to this study.

## Authorship statement

Conceptualized, wrote first draft, gathered MRI images, wrote figure legends, and edited subsequent drafts, and revised the manuscript, edited, and reviewed first and revised submission manuscript: M.I.B.G.. Histopathology, edited and reviewed the final draft, obtained reports and details about STAMP DNA sequencing data and NIH methylation data, created parts of [Figure 3](#) in the revised manuscript, edited and reviewed first and revised submission manuscript: J.J.N.. Re-analyzed DNA sequencing data, obtained, and analyzed RNA sequencing data, generated all data for the revision [Figure 2](#), created [Figure 2](#) and Tables S1–3 in the revised manuscript, revised and edited the manuscript, edited, and reviewed revised submission manuscript: Y.L.X.. Created [Figure 1](#) in the original submission, wrote first draft, wrote figure legends, and edited subsequent drafts, reviewed first and revised submission manuscript: E.A.N.. Created [figure 3](#) in the original submission (clinical trials search), reviewed first and revised submission manuscript: S.A.. Consulted in re-analysis of DNA sequencing data and analyses of RNA sequencing data, provided methods support, assisted with [Figure 2](#) in the revised manuscript, reviewed the revised manuscript: Z.P.F.. Acquired tumor tissue, organized, and reported patient data, acquired IHC, reviewed drafts, reviewed first and revised submission manuscript: E.N.. Organized RNA sequencing, provided patient report updates, reviewed first and revised submission manuscript: A.P.. Organized data, reviewed first, and revised submission manuscript: C.A.G.. Histopathology support, reviewed first and revised submission manuscript: H.V.. Gathered and interpreted MRI, reviewed first, and revised resubmission manuscript: KWY. Conceptualization, reviewed first and revised submission manuscript: G.A.G.. Conceptualization, provided tissue and patient data, gathered MRI, assembled parts of [Figure 1](#) in the revised manuscript, and edited subsequent drafts, reviewed the final first submission, and subsequently revised resubmission manuscript: L.M.P.. Conceptualization, organized, and supervised data acquisition, created parts of [Figures 1–3](#) in the revised manuscript, created [Figure S1](#), inquired molecular analyses, finalized [Figures](#), edited drafts and final manuscript, reviewed first and revised submission manuscript: C.K.P..

## Acknowledgments

We thank Pauline Chu for image scanning; Christine Plant for editing; Dr. Michael Olson (U. Toronto) for advice on the CDC42BPA exon structure; Stanford Molecular Pathology lab and Dr. Iny Jhun and Dr. Rebecca Rojansky for information about the fusion protein. We thank the National Cancer Institute and Dr. Ken Aldape and Dr. Zied Abdullaev for the DNA methylation profiling.

## Affiliations

Department of Neurosurgery, Stanford University School of Medicine, Palo Alto, California, USA (M.I.B.G., Y.L.X., E.A.N., S.A., E.N., A.P., C.A.G., L.M.P., C.K.P.); Division of Neuropathology, Department of Pathology, Stanford University School of Medicine, Palo Alto, California, USA (J.J.N., H.V.); The Australian

National University Bioinformatics Consultancy, John Curtin School of Medical Research, The Australian National University, ACT 2600, Australia (Z.-P.F.); Department of Neurosurgery, Duke University School of Medicine, Durham, NC 27710, USA (G.A.G.); Department of Radiology, Stanford University School of Medicine, Palo Alto, California, USA (K.W.Y.); Division of Pediatric Neurosurgery, Lucile Packard Children's Hospital, Palo Alto, California, USA (L.M.P.)

## References

- Figarella-Branger D, Reuss DE, Solomon DA, Varlet P, Gessi M, von Deimling A. Desmoplastic Infantile Ganglioglioma/Astrocytoma. In: Edited by the *WHO Classification of Tumours Editorial Board. Central nervous system tumours*. Lyon (France). WHO Classification of Tumours, International Agency for Research on Cancer, 5th ed. 2021; vol. 6.
- Hummel TR, Miles L, Mangano FT, Jones BV, Geller JI. Clinical heterogeneity of desmoplastic infantile ganglioglioma: A case series and literature review. *J Pediatr Hematol Oncol*. 2012;34(6):e232–e236.
- Blessing MM, Blackburn PR, Balcom JR, et al. Novel BRAF alteration in desmoplastic infantile ganglioglioma with response to targeted therapy. *Acta Neuropathol Commun*. 2018;6(1):118.
- Gessi M, Zur Muhlen A, Hammes J, et al. Genome-wide DNA copy number analysis of desmoplastic infantile astrocytomas and desmoplastic infantile gangliogliomas. *J Neuropathol Exp Neurol*. 2013;72(9):807–815.
- Tauziède-Espariat A, Beccaria K, Dangouloff-Ros V, et al; RENOCLIP-LOC. A comprehensive analysis of infantile central nervous system tumors to improve distinctive criteria for infant-type hemispheric glioma versus desmoplastic infantile ganglioglioma/astrocytoma. *Brain Pathol*. 2023;33(5):e13182.
- van Tilburg CM, Selt F, Sahn F, et al. Response in a child with a BRAF V600E mutated desmoplastic infantile astrocytoma upon retreatment with vemurafenib. *Pediatr Blood Cancer*. 2018;65(3):e26893–e26896.
- Zhang J, Wu G, Miller CP, et al; St. Jude Children's Research Hospital–Washington University Pediatric Cancer Genome Project. Whole-genome sequencing identifies genetic alterations in pediatric low-grade gliomas. *Nat Genet*. 2013;45(6):602–612.
- Birch JL, Strathdee K, Gilmour L, et al. A novel small-molecule inhibitor of MRCK prevents radiation-driven invasion in glioblastoma. *Cancer Res*. 2018;78(22):6509–6522.
- Jones DT, Kocialkowski S, Liu L, et al. Tandem duplication producing a novel oncogenic BRAF fusion gene defines the majority of pilocytic astrocytomas. *Cancer Res*. 2008;68(21):8673–8677.
- Tan I, Cheong A, Lim L, Leung T. Genomic organization of human myotonic dystrophy kinase-related Cdc42-binding kinase alpha reveals multiple alternative splicing and functional diversity. *Gene*. 2003;304:107–115.
- Haas BJ, Dobin A, Ghandi M, et al. Targeted in silico characterization of fusion transcripts in tumor and normal tissues via FusionInspector. *Cell Rep Methods*. 2023;3(5):100467.
- Capper D, Jones DTW, Sill M, et al. DNA methylation-based classification of central nervous system tumours. *Nature*. 2018;555(7697):469–474.
- Kim P, Tan H, Liu J, et al. FusionGDB 2.0: fusion gene annotation updates aided by deep learning. *Nucleic Acids Res*. 2022;50(D1):D1221–D1230.
- Hu X, Wang Q, Tang M, et al. TumorFusions: an integrative resource for cancer-associated transcript fusions. *Nucleic Acids Res*. 2018;46(D1):D1144–D1149.
- Wang AC, Jones DTW, Abecassis IJ, et al. Desmoplastic infantile ganglioglioma/astrocytoma (DIG/DIA) are distinct entities with frequent BRAFV600 mutations. *Mol Cancer Res*. 2018;16(10):1491–1498.